ELSEVIER

Brain Research 948 (2002) 33–46

BRAIN RESEARCH

www.elsevier.com/locate/bres

Research report

Activation and inhibition of native neuronal alpha-bungarotoxin-sensitive nicotinic ACh receptors

Vladimir V. Uteshev, Edwin M. Meyer, Roger L. Papke*

Department of Pharmacology and Therapeutics, University of Florida College of Medicine, Box 100267 JHMHSC, 1600 SW Archer Rd., University of Florida, Gainesville, FL 32610-0267, USA

Accepted 21 February 2002

Abstract

Tuberomammillary histamine neurons (TM) of the posterior hypothalamus exclusively express alpha-bungarotoxin (αBgt) sensitive nicotinic receptors, providing a unique model system for studying physiological properties of native α7-like receptors. Here the properties of αBgt-sensitive receptors were investigated using the patch-clamp technique and rapid application of acetylcholine (ACh) or the α7-selective agonists, 3-(4-hydroxy,2-methoxybenzylidene)anabaseine (4OH-GTS-21), and choline. Alpha-Bgt-sensitive receptor responses to rapid application of high agonist concentrations were characterized by a transient current which rapidly decayed in a voltage-independent concentration-dependent manner to a relatively sustained slow current. Upon agonist removal, current persisted for several milliseconds (or longer) and increased above the level of the slow current (rebound). Lower agonist concentrations did not produce a rebound. Our analysis suggests that the current rebound represents a recovery phase from a low potency inhibition. This inhibition was voltage-dependent for ACh and choline but voltage-independent for 4OH-GTS-21. A slow form of desensitization was present which was relatively agonist-independent and was faster than the rate of 4OH-GTS-21 unbinding. Kinetic analysis revealed that the concentration dependence of the transient response amplitudes was compromised by solution exchange; net charge measurements over the late response phases were chosen as an alternative measure of concentration/response function. Our data suggest that low agonist concentrations can evoke a prolonged or tonic-like receptor activation. Functioning in this modality, receptors would regulate calcium homeostasis over a narrow, but therapeutically important, range of intracellular calcium concentrations. This could then provide the basis for cytoprotective effects of 4OH-GTS-21 and other nicotinic agonists, mediating trophic and neuromodulatory functions.

Theme: Neurotransmitters, modulators, transporters, and receptors

Topic: Acetylcholine receptors: Nicotinic

Keywords: Acetylcholine; Choline; GTS-21; α-Bungarotoxin; Tuberomammillary nucleus; Desensitization

1. Introduction

The α-bungarotoxin (αBgt) sensitive nicotinic receptor represents a class of low-affinity nicotine binding sites found in the brain in roughly equal abundance to the high-affinity nicotine binding sites but with a distinctly different pattern of distribution [6]. As a result of cloning the α7 gene product, it has become clear that αBgt binding sites likely represent functional receptors that are homomeric pentamers of that subunit [7].

Brain α7-type receptors have been identified at presynaptic or extrasynaptic sites, and several reports have been published of presynaptic effects evoked by relatively low concentrations of nicotinic agonists and sensitive to block by αBgt [10,17]. While these presynaptic receptors have not been amenable to detailed electrophysiological study, putative postsynaptic or somatic α7-like receptors have been identified in a few ex vivo models. For example, nicotinic αBgt-sensitive α7-like receptor-mediated synaptic currents can be recorded from hippocampal interneurons [2,9]. Unfortunately, in situ preparations cannot be studied with reliable rapid agonist application methods, and acute dissociation of interneurons is problematic because they represent a small percent of the mixed

*Corresponding author. Tel.: +1-352-392-4712; fax: +1-352-392-9696.

E-mail address: rpapke@college.med.ufl.edu (R.L. Papke).

0006-8993/02/$ – see front matter
PII: S0006-8993(02)02946-3

neuronal population dissociated from the slice. While cultured hippocampal neurons have been used successfully to study α7-type nAChR [1,5,20], the expression of somatic α7-like receptors on these neurons requires up to several weeks in culture, and so it is not clear how well they may represent receptors found in the brain.

Tuberomammillary (TM) neurons of the posterior hypothalamus [27] provide an alternative model for the study of these receptors because these neurons express a high density of αBgt-binding sites [6], which represent functional nicotinic receptors. We previously reported that the α-Bgt-sensitive receptors of TM neurons could be activated by a rapid application of acetylcholine (ACh), and DMPP, as well as 4OH-GTS-21 [23,27]. These histaminergic TM neurons can be easily identified after acute dissociation [26]. They respond to a rapid application of high concentration of agonist such as 2 mM ACh or 200 μM 4OH-GTS-21 with a transient current followed by a sustained current of small amplitude. ACh- and 4OH-GTS-21-mediated responses in TM neurons can be completely blocked by 0.1–1 μM αBgt, confirming that these responses are mediated by αBgt-sensitive α7-like receptors [23,27].

In the present study we provide a detailed characterization of the α7-type receptor responses of TM neurons to the α7-selective agonist, 4OH-GTS-21, and the endogenous agonists, ACh and choline. We show that low (patho)physiological concentrations of nicotinic agonists induce in αBgt-sensitive receptors a slowly desensitizing receptor activation that may lead to a prolong calcium influx which in turn can potentially be cytoprotective and regulatory for histamine release. An improved analysis of solution exchange around the neuron confirms our previous hypothesis that the peak responses to the application of high concentrations of agonist occur during the concentration ramp. We discuss the implication of this and other concentration-driven processes for interpretation of α7-receptor-mediated responses. Through the use of recording conditions that permit us to study both inward and outward currents, we were able to characterize voltage-dependent inhibition by ACh and choline that seemed to be distinct from the fast desensitization process that also limits the responses to high agonist concentrations. Once agonist was removed, there was a relief of this voltage-dependent inhibition, which appeared as a rebound above the level of current obtained in the presence of the high agonist concentration.

A detailed analysis of the experimental agonist 4OH-GTS-21 concentration–response function indicated that responses to this agent differed significantly from the responses to ACh and choline in regard to voltage dependence and kinetics. The data may afford important insight into the potential clinical use of this agent and the related compound GTS-21. The α7 nicotinic receptor is a target for recently developed memory-enhancing and neuroprotective agents such as GTS-21 and 4OH-GTS-21 [16,19], which are being evaluated clinically for the treatment of Alzheimer's disease [14]. These compounds are reported to be selective partial agonists of α7 nicotinic receptors [18] and have the capacity to induce a variety of calcium-sensitive intracellular transduction processes that differ depending on the agonist concentration [16].

2. Materials and methods

2.1. Chemicals

4OH-GTS-21 was synthesized and provided by Taiho Pharmaceuticals (Tokushima, Japan). All other chemicals were obtained from Sigma (St. Louis, MO).

2.2. Electrophysiology

The brains of 1–6-week-old Sprague–Dawley rats (Charles Rivers, Wilmington, MA) were removed following decapitation and placed for 1–2 min in ice-cold oxygenated Kreb's solution of the following composition (in mM): NaCl 125, KCl 3.5, KH_2PO4 1.2, $MgCl_2$ 1.3, $CaCl_2$ 1.8, $NaHCO_3$ 25, glucose 10 and HEPES (NaOH) 10 (pH 7.4) when bubbled with carbogen (95% O_2 and 5% CO_2). Two to three slices of 300–400 μm thickness containing the tuberomammillary nucleus were prepared using a Vibratome. Slices were then left for 15–20 min in the oxygenated Kreb's solution to equilibrate extracellular ionic contents. Slices prepared for the acute dissociation experiments were then transferred to 20 ml of oxygenated Kreb's solution, and 0.5–1 mg/ml papain (papaya latex in crude form, 1.9 units/mg, Sigma Chemical Co., St. Louis, MO) was added for 1.5 h at room temperature. After papain treatment, slices were washed and could be maintained at room temperature for up to 10 h (bubbled with carbogen).

2.3. Acutely dissociated neurons

Slices were placed at room temperature in an experimental physiological solution of the following composition (in mM): NaCl 150, KCl 5, $CaCl_2$ 2, HEPES 10, glucose 10 (pH 7.4). Neurons from tuberomammillary nucleus were isolated by mechanical dissociation using two fire-polished glass needles at the beginning of each experiment. Putative histamine neurons were distinguished based on their location within the slice as well as on morphological (size and shape) and electrophysiological (profound I_A and I_h currents) properties [26,27]. All neurons that were identified as putative histamine neurons demonstrated current responses upon fast applications of nicotinic agonists. Recording patch-clamp pipettes with the resistance of 2–3 MΩ were polished and filled with the following intracellular solution (in mM): CsCl 40, CsF 100, HEPES 10 (pH 7.3). Data were acquired at 5 or 10

kHz and analyzed using pClamp8 software (Axon Instruments).

To deliver nicotinic agonists to the cells, a double-barreled application pipette was used as described previously [23]. The double-barreled application pipette was built of two fused application tubes (World Precision Instruments, Inc., O.D.=0.35 mm, I.D.=0.25 mm), firmly mounted on a Burleigh piezoelectric LSS-3200 solution switcher, and controlled via a computer (pClamp8, Axon instruments). One tube provided a continuous flow of bath solution, and the other could be changed among various experimental agonist solutions. Solutions were then exchanged via the rapid movement of the application pipette. Voltage steps used to control the solution switcher were generated by the data acquisition program and conditioned by a filter circuit as previously described [13].

Tetramethylpiperidine (TMP) is a potent use-dependent inhibitor of neuronal nAChR [8]. In some experiments the wash barrel of the application system was filled with a solution that contained 3 μM 4OH-GTS-21, and the application barrel contained a mixture of 3 μM 4OH-GTS-21 and 0.5 mM TMP. The neuron was then introduced manually into the flow of 3 μM 4OH-GTS-21, and after a steady-state whole-cell current was achieved, solution was rapidly changed to 3 μM 4OH-GTS-21 plus 0.5 mM TMP using our application system, so that the solution exchange rates could be estimated.

3. Results

We previously reported that acutely dissociated histaminergic neurons of the TM nucleus (Fig. 1) exhibited robust nicotinic receptor-mediated responses to ACh and the α7-selective agonists, choline and 4OH-GTS-21. These responses were totally blocked by α-Bgt, further confirming these cells as an excellent system for the study of neuronal α7-type nAChR [23]. We sought to extend our characterization of the neuronal responses to the selective agonist 4OH-GTS-21 through an analysis of the time and concentration dependence of the agonist-evoked responses.

3.1. Description of an α7-mediated response to 4OH-GTS-21

As shown in Fig. 2, the responses to 4OH-GTS-21 application may be characterized by as many as three phases, depending on the agonist concentration applied. With the application of high concentrations, there were typically three distinct phases of the response, which we will refer to as the 'transient' current and the 'slow' current, which occurred during the agonist application, and the 'delayed' current, which occurred after agonist was removed. As shown in the figure, with the application of a relatively low concentration of agonist (e.g. 3 μM), no synchronized peak response could be easily defined; the current increased slowly over the few hundred milliseconds to what seemed to be a sustained level, corresponding to a slow current. However, with increasing agonist concentration, there was a clear, early peak-current response. Both the amplitude and the transient nature of this phase of the response were enhanced in a concentration-dependent manner. The transient nature of the peak current presumably was due to the fast desensitization characteristic of α7-mediated responses to the application of high concentration of agonist.

Following the transient currents, responses decayed and approached a variable level of slow current (Fig. 2). The level of the slow current was highest when low to intermediate concentrations of agonist were applied and

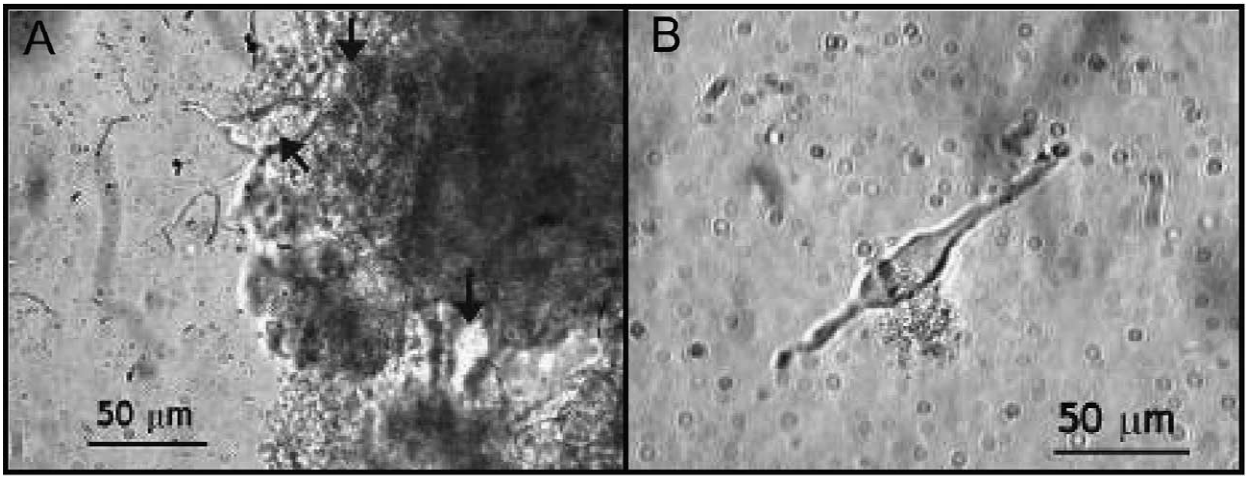

Fig. 1. (A) Three neurons (indicated by arrows) have been partly dissociated from the TM nucleus of the posterior hypothalamus. All three neurons are readily accessible for patch clamp experiments. The left most neuron represents the best choice of three. (B) An example of a completely dissociated bipolar TM neuron is shown. Both partly and completely dissociated TM neurons were used in our experiments. However, partly dissociated neurons were preferred as they supported more stable electrophysiological whole-cell recordings.

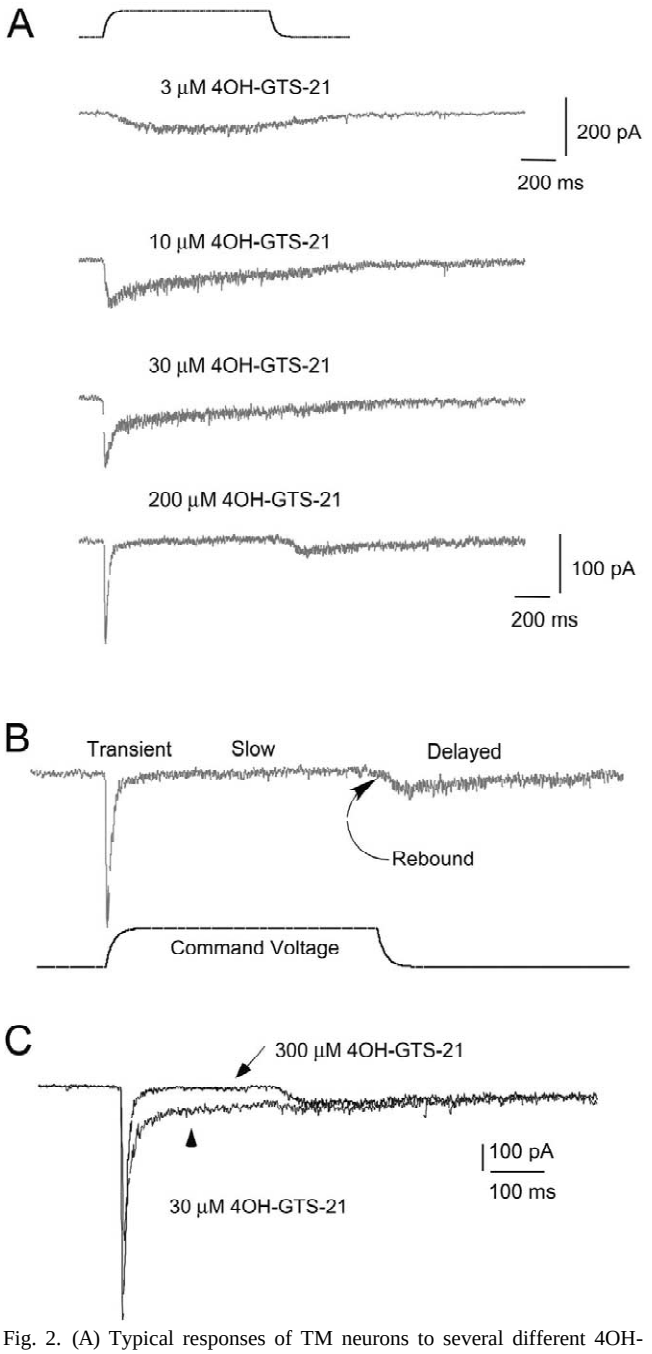

Fig. 2. (A) Typical responses of TM neurons to several different 4OH-GTS-21 concentrations are shown. The 10-, 30-, and 200-μM responses were obtained from the same cell. The response to 3 μM was recorded from a different neuron and then scaled, based on the relative amplitude of the responses to 30 μM 4OH-GTS-21 obtained from that neuron, compared to the 30 μM response of the other cell. The holding potential was −80 mV. A command signal to the piezoelectric solution switcher is shown above the responses. Note that the actual agonist application was much more rapid than the voltage command [23]. (B) Illustration of the multiple phases of neuronal α7 receptor response to a high concentration of 4OH-GTS-21. The response to 200 μM 4OH-GTS-21 from panel A is shown on a somewhat expanded scale to illustrate the three phases of the response: the transient, the slow, and the delayed current. Also labeled is the rebound current, which occurred at the boundary of the slow and delayed current. (C) Superimposition of the responses of a single TM neuron to 30 and 300 μM 4OH-GTS-21. The higher concentration response showed a large and more rapid peak but a much smaller slow current. Also note that the lower concentration response showed virtually no rebound in the transition from slow to delayed current.

was lower when high concentrations of agonist were applied. Currents relaxed back to baseline after the agonist was removed. The delayed current evoked by 4OH-GTS-21 (Fig. 2B) took several hundred milliseconds to return to baseline. This delayed current presumably represented sustained activation of the channels due to agonist that remained bound after the agonist-containing solution was removed. The amount of delayed current appeared to be saturated at a concentration of approximately 30 μM 4OH-GTS-21 (Fig. 2C).

At concentrations higher than 30 μM 4OH-GTS-21, there was less slow current, and upon removal of the high concentration agonist solution, there was an increase in current up to that seen with the 30 μM 4OH-GTS-21 delayed response, which was apparently the maximum delayed current response (see the 300 μM 4OH-GTS-21 response in Fig. 2C). We refer to the increase in the delayed current to a level above that of the slow response as 'rebound' current. Such rebound currents were only observed at agonist concentrations higher than 30 μM for the 4OH-GTS-21-evoked responses. As shown in Fig. 2C, delayed currents mediated by 30 and 300 μM 4OH-GTS-21 appeared to be very similar. This suggests an existence of low potency receptor inhibitory site(s). The low potency inhibition became effective at concentrations roughly over 30 μM 4OH-GTS-21 (Fig. 2A and C) which was equivalent to approximately 300 μM ACh (see Fig. 6). The rebound current therefore appeared to represent the relaxation of the low potency inhibition caused by the higher agonist concentration.

3.2. Voltage dependence of the 4OH-GTS-21 evoked responses

We previously reported that the kinetics of the fast transient component of 4OH-GTS-21 evoked responses were not affected by transmembrane voltage [23]. In the present experiments, we also investigated the potential voltage dependence of the slow and delayed currents. Since recordings were made in the absence of extracellular magnesium, we saw relatively little inward rectification, which has been reported to be extracellular magnesium dependent [4], and we were able to record responses over a wide range of voltage. As shown in Fig. 3, 4OH-GTS-21-evoked responses recorded at hyperpolarized and depolarized potentials showed essentially identical kinetic features ($n>8$), suggesting that in the case of 4OH-GTS-21 the low potency inhibition was voltage-independent.

3.3. Transient currents and solution exchange

In Fig. 4A we show the relationship between the amplitude of the transient current and the concentration of 4OH-GTS-21 applied. Note that when the peak current amplitudes are plotted as a function of the agonist con-

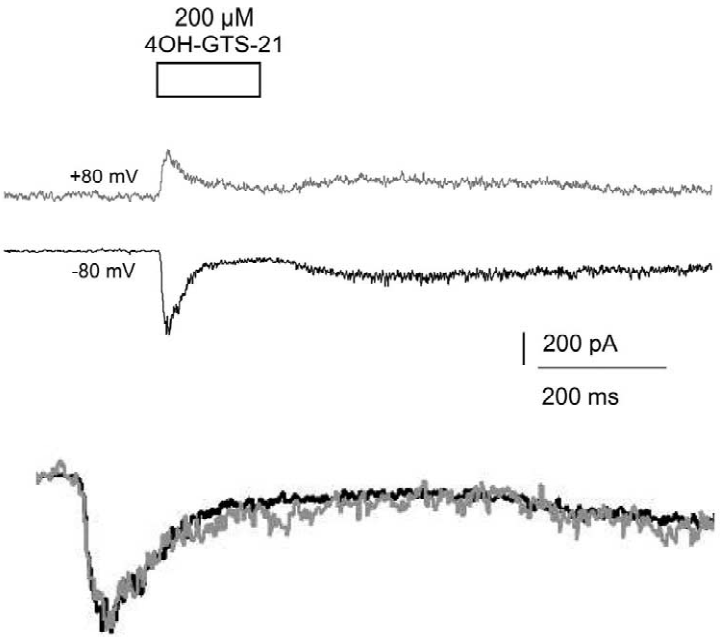

Fig. 3. Two responses from a TM neuron to the application of 200 μM 4OH-GTS-21 obtained at either the standard holding potential of −80 mV or the depolarized potential of +80 mV. As shown in superposition at the bottom of the figure, the kinetics of the 4OH-GTS-21 responses were virtually insensitive to voltage. At both voltages a rebound was present at the transition from the slow to delayed current. Note that the absolute amplitude of the peak current was somewhat less at +80 compared to −80, consistent with the reversal potential >0 mV (data not shown). In order to compare kinetics, the response obtained at +80 mV was scaled and inverted so that the peak responses coincided.

centration applied, the graph appears to be monotonic (Fig. 4A). However, the fast desensitization of the responses led us to question whether there is a valid association between this measure of functional response and the concentration used to stimulate the cell [23,24]. If peak currents occur before full solution exchange, the determination of values such as the EC_{50} for the analysis of transient currents would be invalid. Open-tip recordings are commonly used for the comparison between solution exchange and a physiological response [20]. However, an open-tip recording does not reproduce the geometry of the whole-cell configuration and thus the dynamics of the solution exchange around a cell. An open-tip recording, which essentially represents a solution exchange at a point source, would likely underestimate the time required for the solution interface to cross the surface of a large cell like a TM neuron. In order to better estimate solution exchange relative to the timing of peak responses in our system, we developed a method for the cell itself to serve as the reporter of the solution-exchange kinetics. Responses to 200 μM 4OH-GTS-21 were first obtained with the agonist in normal recording solution (150 mM Na). The experimental application solution was then replaced with one that contained 200 μM 4OH-GTS-21 and only 75 mM sodium, and data was obtained from the same cell with the same stimulation protocol. Recording responses in 75 mM sodium had the effect of reducing the driving force so that the slow current fell to zero (Fig. 4B). If the peak of the evoked response occurred when full solution exchange was completed, then the reduced driving force should have had equal impact on both the peak and the slow phase of the response. However, when the peaks were normalized, there was a far greater effect on the slower phase of the response than on the peak itself (Fig. 4C). The driving force during the peak of the response was reduced by only 40–57%, suggesting that the agonist concentration at the time of the peak was probably no more than 100 μM (Fig. 4D).

To obtain another independent estimate of the solution exchange rate using a TM neuron as a detector, we employed 0.5 mM TMP, a fast use-dependent blocker of nicotinic receptor ion channels [8]. Fig. 4E demonstrates that the TMP-induced block occurred within the first 10 ms of 0.5 mM TMP application. Data from multiple experiments indicated that complete block with this high concentration of TMP was achieved with a time constant of 7.4±0.4 ms (n=7). In comparison, the average time of the peak responses to 200 μM 4OH-GTS-21 was only 5.6±0.7 ms (n=6). Given that solution exchange had a time constant of 7.4 ms, we calculated the fractional exchange at 5.6 ms to be $(1-e^{-5.6/7.4})$ or 50%. This was consistent with the results of the sodium solution exchange experiment, suggesting that in response to the application of agonists at high concentrations, the decay of the peak currents began before solution exchange could be completed.

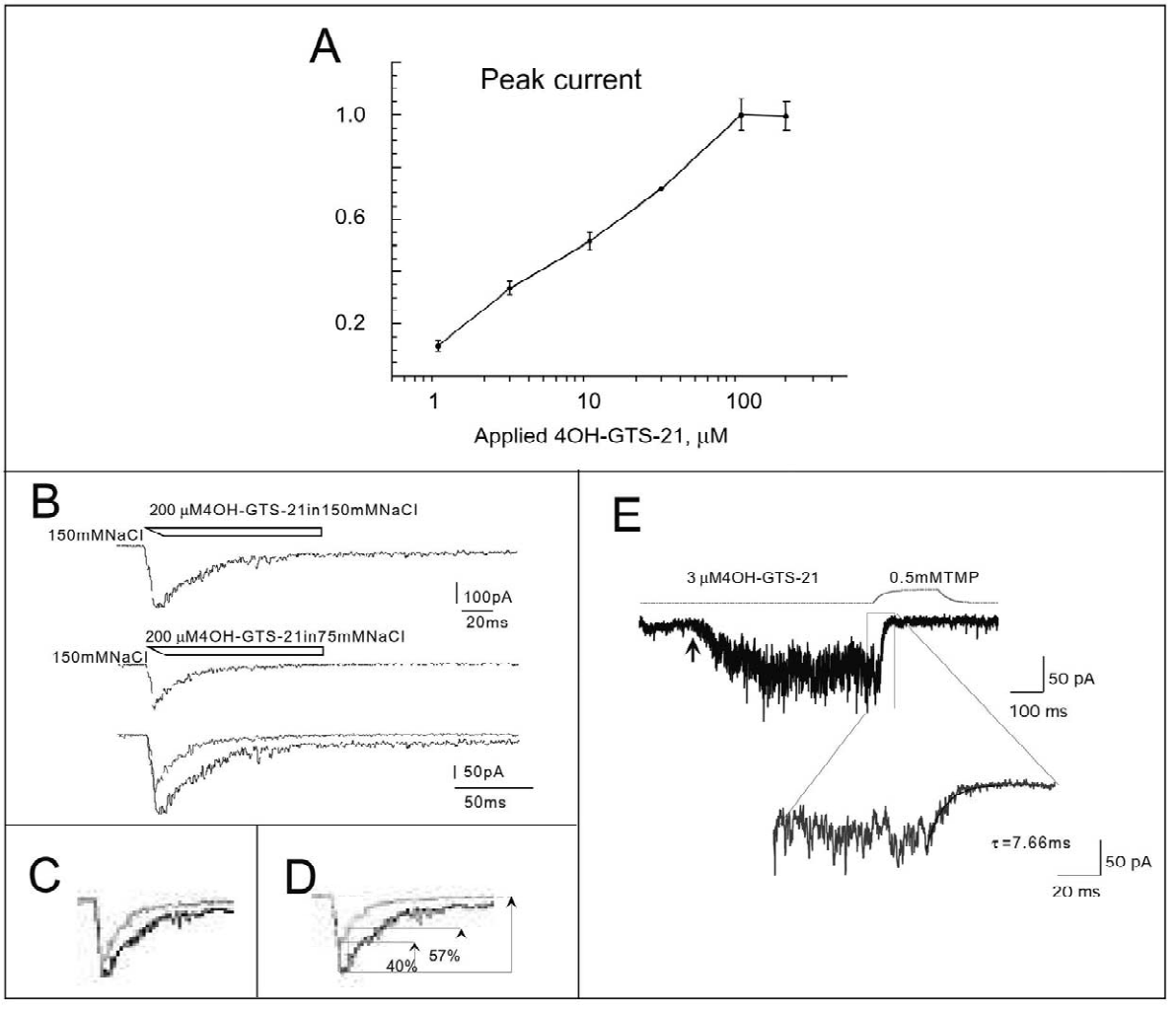

Fig. 4. (A) The apparent concentration–response curve for transient current amplitudes plotted against the agonist concentration applied. (B) To evaluate the kinetics of peak response in relation to the kinetics of solution exchange, 200 μM 4OH-GTS-21 was applied in either normal sodium concentration (upper trace) or at 50% normal concentration (75 mM, middle trace). As shown in the overlay (bottom trace), the decrease in sodium was sufficient to decrease the driving force on receptor-mediated current to zero, so that while full solution exchange was achieved during the phase of sustained current in normal sodium concentration, there was no net current in the low sodium solution. (C) Normalizing the two responses to the peak current revealed differences in response shapes, indicating a non-instantaneous solution exchange since the peak responses were relatively unaffected compared to the slower phases as the driving force approached zero. (D) Note that the peak current response in the low sodium solution was 73% of the response in the normal sodium solution, illustrating how peak responses to the application of high agonist concentrations occurred well before solution exchange was complete. A comparison of the peak responses recorded at different sodium concentrations and the same 4OH-GTS-21 concentration allowed us to estimate the true concentration of 4OH-GTS-21 to be 80–115 μM at the time of the response peak (i.e. 40–57% of full solution exchange, see text). (E) The recording electrode with a TM neuron attached to its tip was brought manually into the flow containing 3 μM 4OH-GTS-21. After a steady-state whole-cell response was obtained, a solution containing a mixture of 3 μM 4OH-GTS-21 and 0.5 mM TMP was applied to the neuron, using our application system to replace the 3 μM 4OH-GTS-21. The rate of the current block was then estimated (see text). The holding potential was −80 mV.

3.4. Concentration/dose–response functions for α7 nAChR agonists

Since the fast kinetics of the αBgt-sensitive transient responses indicated that there was not a valid association between concentration and response in the higher concentration range, we propose that net charge over the late response phases where the solution exchange is complete is a better a measurement of response than peak current. A similar analysis has been applied to α7 receptor-mediated responses in cultured hippocampal neurons [20] and α7 receptors expressed in *Xenopus* oocytes (Papke and Papke, submitted for publication).

For the measurement of net charge evoked by 4OH-GTS-21, 1-s agonist applications were employed. In order to evaluate the impact of the transient currents on the net charge measurements, separate charge calculations were made for the first 500 ms and the last 500 ms of the

responses. Data were obtained from 14 TM neurons, and in each case responses to applications of 30 μM 4OH-GTS-21 were measured and used to normalize the responses to other concentrations and thus control for the variability in the single cell responses.

Net charge was calculated for both the first 500 ms and the second 500 ms of 1-s applications, and bell-shaped concentration-dependence plots were obtained (Fig. 5). Presumably this was because both the positive (i.e. activating) and negative (i.e. desensitizing or inactivating) concentration-dependent factors were reflected in the analysis of net charge. Maximal charge measurements were seen with the application of 4OH-GTS-21 at concentrations less than or equal to 30 μM, and higher concentrations clearly produced less net response. When looking at the last 500 ms, it appeared that the largest net charge responses were seen with lower concentrations than for the first 500 ms. However, it should be noted that at the higher concentrations, the first 500 ms contained the transient current, which actually represented the response to lower concentrations than what was applied (i.e. the plotted value). When only the slow current was considered, 3 μM 4OH-GTS-21 seemed most effective for activating the receptor. The data for the 0–500 ms net charge response in the concentration range from 1 and 30 μM 4OH-GTS-21 was fit to the Hill equation (not shown), which gave an estimated EC_{50} of 1.6±0.6 μM 4OH-GTS-21 with a Hill coefficient $n=2.6\pm0.2$. Interestingly, these values agreed well with those estimated by net charge analysis of rat α7 receptors expressed in *Xenopus* oocytes (EC_{50} of 1.6±0.2 μM, $n=2.1\pm0.4$, Papke and Papke, submitted for publication).

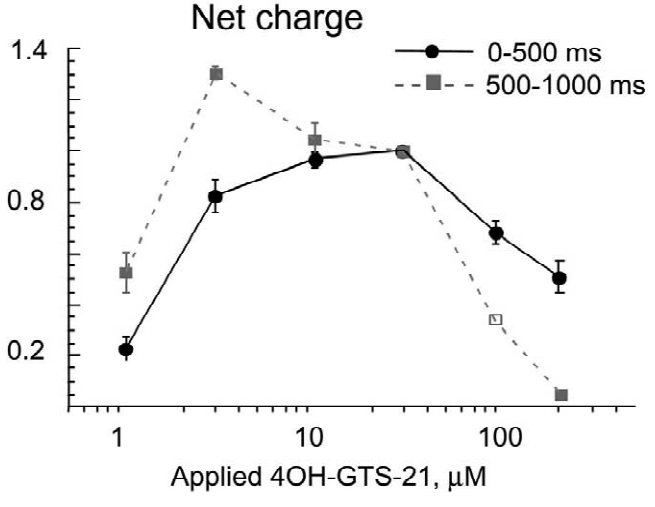

Fig. 5. A bell-shape curve characterized the concentration dependence of responses to 4OH-GTS-21 when net charge was estimated over the first 500 ms (circles) and the last 500 ms (squares) of a 1-s response. When the transient phase of responses was excluded from response measurements, the influence of incomplete solution exchange on the concentration–response dependence could be minimized or avoided. The bell shape of the concentration–response dependence suggests the existence of a range of agonist concentrations that is optimal for receptor activation. The open square corresponds to $n=1$; filled circles and squares correspond to $n=5$–6.

3.5. Comparison of α7-mediated responses to ACh choline and 4OH-GTS-21

We compared the responses of TM neuronal α7-type receptors to the selective agonist 4OH-GTS-21 to the responses evoked by low and high concentrations of the two endogenous agonists, ACh and choline. In regard to the peak transient and slow currents, responses to these agonists recorded at standard holding potentials differed mainly in their concentration dependence. While maximal peak currents could be obtained with the application of 200 μM 4OH-GTS-21, responses of similar amplitude required the application of 2 mM ACh or 10–20 mM choline (Fig. 6). Note that the rise and decay rates of the ACh and choline-evoked currents were essentially identical to those of the 4OH-GTS-21-evoked responses in the same cells (Table 1). However, as shown in Fig. 6, the decay of the choline-evoked delayed current was faster than the ACh-evoked delayed current, which in turn was much faster than that of the 4OH-GTS-21-evoked delayed current (Table 2).

3.6. Voltage dependent and independent processes are revealed in the responses to ACh

We investigated the effects of transmembrane voltage on the responses to high and low concentrations of ACh and choline. While as previously reported [23], voltage did not affect the kinetics of the fast transient current, there was a significant effect of voltage on the level of the slow current. Relative to the amplitude of the transient current, there was less slow current when cells were held at negative potentials. Fig. 7A illustrates the effects of 200 μM and 2 mM ACh on the same TM neuron. Note that no current rebound was observed when 200 μM ACh was applied. However, when 2 mM ACh was applied, the rebound was present at negative holding potentials but absent at high positive membrane voltages, corresponding to a significantly higher slow current relative to the transient current (see Table 3).

The averaged decay time constant of 2 mM ACh-mediated fast transient responses at −80 mV was 10.6±1.2 ms, $n=7$. The time constant of the onset of low potency voltage-dependent inhibition was determined by fitting the difference-current, calculated by subtraction of traces recorded at positive and negative membrane voltages (Fig. 7C). This voltage-dependent feature had a time constant of 54.5±2.7 ms, $n=4$, when 2 mM ACh was used as agonist, much slower than the fast voltage-independent desensitization. Therefore, it appeared that the low potency voltage-

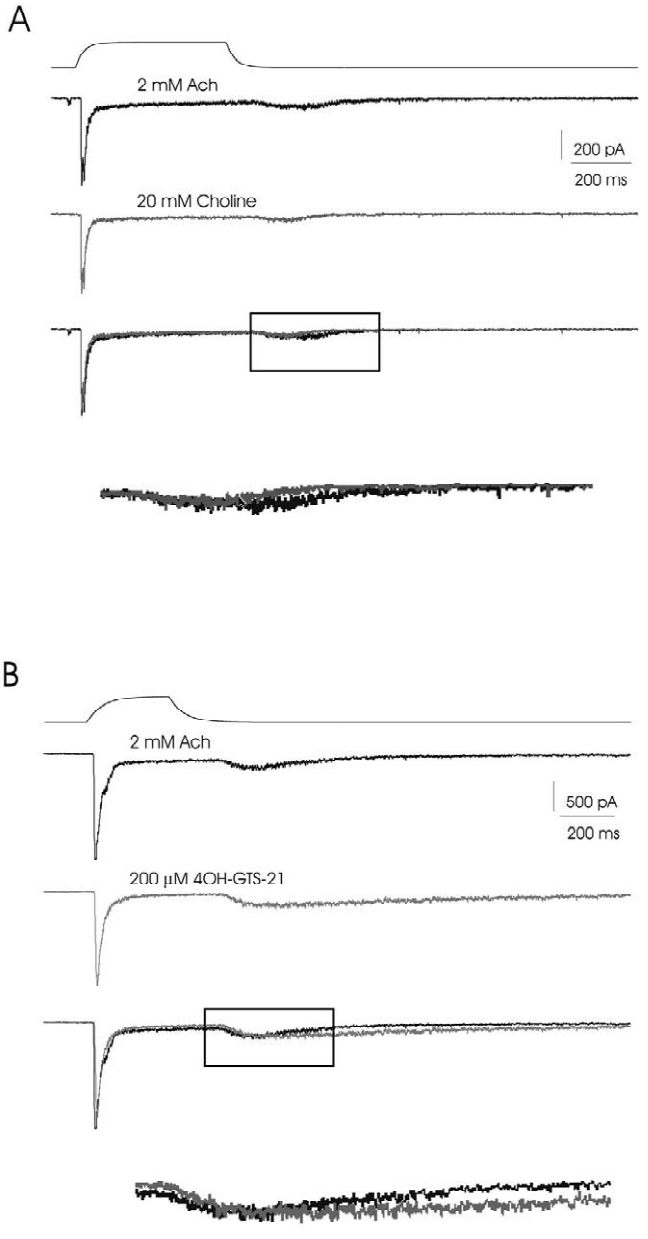

Fig. 6. (A) Response of a TM neuron to high concentrations of ACh (top trace) and choline (second trace). Note that 20 mM choline was required to obtain a transient current response comparable to that evoked by 2 mM ACh. The third trace is the superimposition of the 2 mM ACh and 20 mM choline responses. The peaks and slow currents were essentially identical. However, the delayed phase of the choline response decayed more rapidly than the ACh delayed current (enlarged in insert). (B) Response of a TM neuron to high concentrations of ACh (top trace) and 4OH-GTS-21 (second trace). Note that only 200 μM 4OH-GTS-21 was required to obtain a transient current response comparable to that evoked by 2 mM ACh. The third trace is the superimposition of the 2 mM ACh and 200 μM 4OH-GTS-21 responses. The peaks and slow currents were relatively similar. However the delayed phase of the 4OH-GTS-21 response decayed much more slowly than the ACh delayed current (enlarged in insert).

dependent inhibition did not contribute significantly to the decay of the fast transient currents (see Table 1). As shown in Fig. 7D, the effects of voltage on the choline-evoked responses were essentially the same as on the ACh-evoked responses. In contrast to the case of 4OH-GTS-21 (Fig. 3), the low potency inhibition for ACh and choline was voltage-dependent. The relief of the low potency voltage-dependent inhibition appeared to be responsible for the rebound above the level of the slow current that occurred when the agonist is removed.

3.7. 'Slow' desensitization

In order to determine whether the duration of a high concentration agonist application affected the amount of activation observed in the rebound and delayed currents, we measured delayed current after varying lengths of agonist application for 4OH-GTS-21 and ACh. As shown in Fig. 8A and B, the amplitude of delayed current progressively decreased as the length of the agonist application increased. This decrease in responsiveness introduced a slow form of desensitization, distinct from the fast desensitization that impacted the transient currents. Although, as noted previously, the decay rates of the delayed currents differed for the two agonists (Fig. 6, Table 2), the rate at which the delayed currents were diminished by prolonged agonist application appeared to be very similar for high concentrations of both ACh and 4OH-GTS-21 (Fig. 8C). Interestingly, for 4OH-GTS-21 in most experiments, the rebound peaks obtained using different application durations lined up in a sequence that could be embraced by a rebound current obtained using a shorter duration (Fig. 8A).

To measure the rates of the recovery from desensitization, we employed a pair-pulse protocol and used concentrations of 4OH-GTS-21 between 3 and 200 μM. For comparison, 2 mM ACh was also used. For 3 μM 4OH-GTS-21, there was no rapid desensitization evident, and the recovery from all forms of desensitization was essentially complete within 1 s after the beginning of the agonist wash (Fig. 9A). Higher 4OH-GTS-21 concentrations, however, drove more receptors into desensitization states, from which recovery occurred with similar time constants in the range of 1100–1200 ms (Fig. 9B). The recovery from desensitization caused by 2 mM ACh was faster than that mediated by a comparably efficacious concentration of 200 μM 4OH-GTS-21, with a time constant of approximately 500 ms. Recovery from 4OH-GTS-21-evoked desensitization was slower than from ACh-evoked desensitization, presumably because 4OH-GTS-21 dissociated more slowly (Fig. 6B), maintaining higher levels of receptor occupancy. Note that in all cases, full recovery was achieved after 40 s of wash, the time between consequent pair-pulse trains.

Table 1
Time constants of current decays

Agonist	Time constant of decay of fast transient current (ms)	Time constant of V-dependent decrease in slow current (ms)
200 μM 4OH-GTS-21	12.3±1.7 (n=11)	n.a.
2 mM ACh	10.6±1.2 (n=7)	54.5±2.7 (n=4)
10 mM Choline	9.65±1.1 (n=9)	20.83±3.24 (n=2)

4. Discussion

Through the use of acutely-dissociated TM neurons (Fig. 1), we have been able to conduct an analysis of brain α7-type receptors, with precise control of agonist concentration and application kinetics. Using improved methods for evaluating solution exchange around the cell, we confirm that α7 receptor responses to high concentrations of agonist achieved their maximal amplitude before a complete solution exchange. This supports the hypothesis that α7-type receptors possess a novel form of concentration-driven kinetics which promotes the synchronization of receptor activation during a steep ramp in concentration change, regardless of whether the ramp is slow, as in an oocyte experiment [24] or rapid, as in the present experiments. We identified three phases in a typical response to a high concentration of agonist which appear to arise from multiple processes that either promote or lessen channel opening. The overall effect of these multiple processes was that, under standard recording conditions, the concentration response function for net charge was bell shaped, even when charge was integrated over the initial portion of current that included the transient current component. Thus maximal transfer of charge into the cell occurred with relatively low concentrations of agonist.

The synchronization of channel activation underlying the fast transient current relaxed to the slow current (Fig. 2A and B). Hence, we saw a fast desensitization during the transient current, while the decay of the slow current was evidently due to another desensitization process. The latter desensitization process could not be observed when high agonist concentrations were used, due to initiation of the low potency inhibition that together with slow desensitization limited slow current. This inhibitory process, which was voltage-dependent for ACh and choline, had kinetics and concentration-dependence which made it distinct from both fast and slow desensitization. It required concentrations of agonist that were higher than those which produced the largest slow current (i.e. roughly over 30 μM 4OH-GTS-21), and based on the analysis of voltage dependence, it had a relatively slow onset. The relaxation of this low potency inhibitory process upon removal of agonist manifested as a rebound. All of these features are consistent with channel block by the agonist. The low potency inhibition was observed with 4OH-GTS-21 at both positive and negative holding potentials and the lack of voltage-dependence in the 4OH-GTS-21 responses was consistent with the observation that, at physiological pH, this agonist was primarily uncharged (Bill Kem, personal communication), and therefore any channel blocking action would be driven by concentration-dependent processes alone.

Table 2
Time constants of rebounds and delayed currents

Agonist	Time constant of rebound current (ms)	Time constant of decay of delayed current (ms)
4OH-GTS-21	29.0±3.2 (n=11)	792.9±151.9 (n=5)
ACh	37.1±4.6 (n=12)	139±14 (n=7)
Choline	28.4±4.0 (n=14)	77.6±8.6 (n=6)

In addition to the difference in the voltage-dependence of rebound currents, we found that responses to 4OH-GTS-21 differed from ACh and choline-evoked responses in two other ways: potency for producing activation, and duration of the delayed currents. 4OH-GTS-21 was ten-fold more potent at evoking maximal transient currents than was ACh, and ACh was ten-fold more potent that choline. This is the same potency ratio which has been previously reported in studies of α7-mediated currents in oocytes [22]. Likewise, a ten-fold potency difference between ACh and choline has been reported for cultured hippocampal neurons [3,20]. The decay rate of the 4OH-GTS-21-evoked delayed currents was roughly five times longer than that of the ACh-evoked delayed currents (Table 2). As previously reported by Mike et al. [20], we noted that, upon removal of agonist, the currents activated by choline decayed roughly twice as fast as did the currents activated by ACh.

In summary, there were three distinct processes which oppose the agonist-dependent activation of α7 receptors in

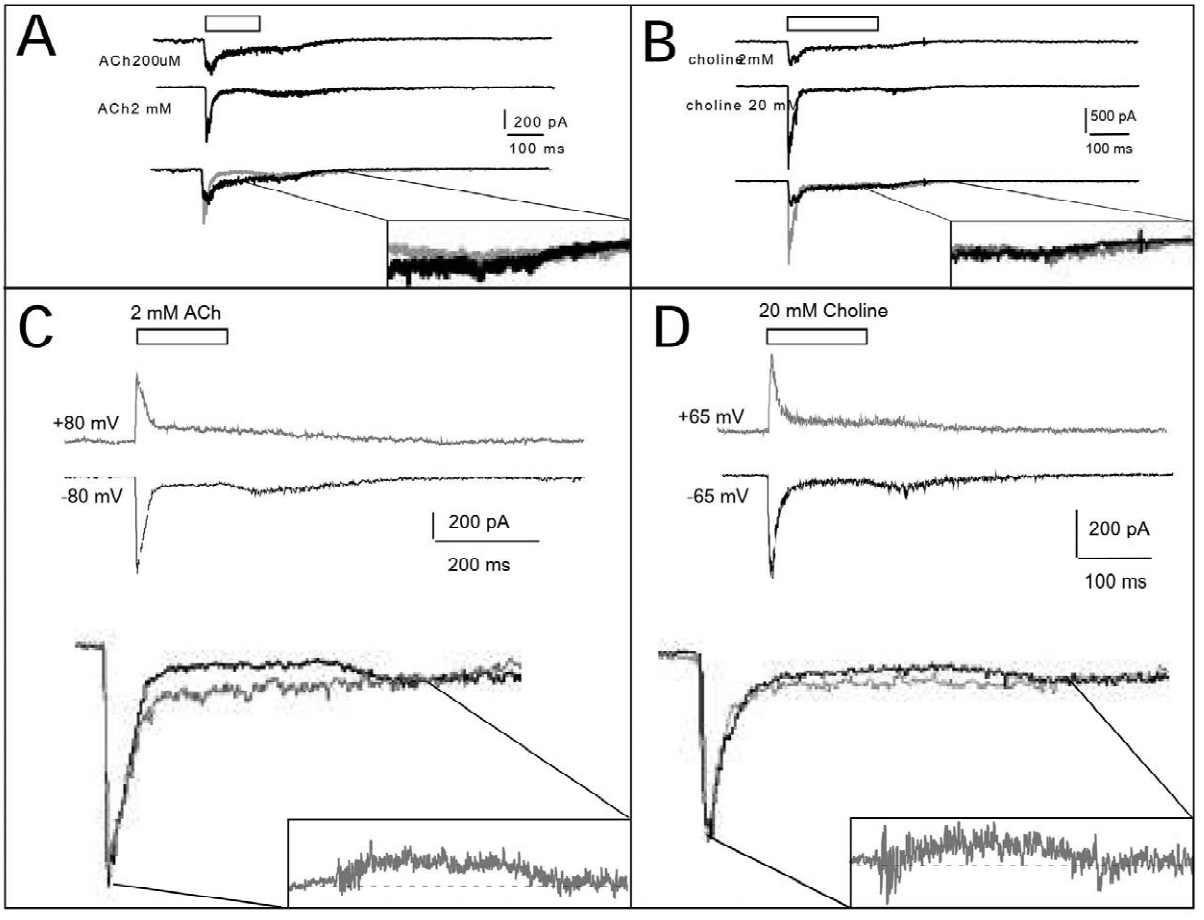

Fig. 7. (A) Multiple phases in the response of a TM neuron to the rapid application of ACh at the standard −80 mV holding potential. Responses to 200 μM (top trace) showed a relatively slow transient current, a substantial slow current, and delayed current without appreciable rebound, similar to the responses to 30 μM 4OH-GTS-21 (see Fig. 2). The application of a ten-fold higher ACh concentration (second trace) sharpened the transient current and resulted in a decreased slow current, producing a rebound current upon agonist removal. Note that a rebound current is apparent at the transition from the slow to the delayed current with the 2 mM ACh-evoked response, but not the 200 μM ACh-evoked response (see insert). (B) Multiple phases in the response of a TM neuron to the rapid application of choline. Responses to 2 mM choline (top trace) showed a relatively slow transient current, a substantial slow current, and delayed current without appreciable rebound. The application of a ten-fold higher choline concentration (second trace) sharpened the transient current and resulted in a small decrease in the slow current, producing a modest rebound current upon agonist removal (see insert). (C) Responses of a TM neuron to the application of 2 mM ACh obtained at either the standard holding potential of −80 mV or at the depolarized potential of +80 mV. As shown in scaled superposition at the bottom of the figure, the slow and delayed phases of the ACh responses were affected by holding potential. Specifically, the slow current was decreased at the negative holding potential, and a rebound at the transition from the delayed to slow current was only present when the cell was held at −80 mV. As previously noted, the absolute amplitude of the peak current was somewhat less at +80 compared to −80 due to the slightly positive (+10 mV) reversal potential and a mild outward rectification, therefore, in order to compare kinetics, the response obtained at +80 mV was scaled and inverted so that the peak responses coincided. The difference-current between the two scaled responses is shown in the insert panel. (D) Responses of a TM neuron to the application of 20 mM choline obtained at either a holding potential of −65 mV or at the depolarized potential of +65 mV. As shown in scaled superposition at the bottom of the figure, the slow and delayed phases of the choline responses were also affected by holding potential. As with the ACh-evoked responses, the slow current was decreased at the negative holding potential and a rebound at the transition from the slow to delayed current was only present when the cell was held at −80 mV. The difference-current between the two scaled responses is shown in the insert panel.

the continued presence of agonist: fast desensitization, slow desensitization, and channel block. Fast desensitization manifested as a form of concentration dependence, such that the probability for channel opening (P_{open}) was greatest on the leading edge of a steep concentration ramp and decayed rapidly as concentration increased further. In addition to this concentration-dependence, fast desensitization was also likely to have some time-dependence that might be described by a first-order rate constant for the conformational change to the desensitized state. It is therefore an impediment to the explicit modeling of α7 responses that the simultaneous changes in P_{open} and agonist concentration that occur during the transient response must somehow be deconvoluted. This may not be an obtainable goal if, regardless of the speed of agonist application, there is always a lower probability of channels being open at the highest agonist concentration than at an intermediate concentration which is achieved earlier on the

Table 3
Voltage dependence of slow currents with ACh and 4OH-GTS-21 currents normalized to respective transient currents

200 μM 4OH-GTS-21		2 mM ACh	
−80 mV	+80 mV	−80 mV	+80 mV
0.080±0.031	0.142±0.049	0.099±0.011	0.225±0.027*

Current amplitudes (±S.E.M., $n=3$) for slow currents calculated as the average current over a 30-ms interval from 130 to 160 ms into the response. In order to normalize the data, the slow currents were expressed as a fraction of the average current during the peak of the same response (i.e. during the first 30 ms of the response, see Fig. 7 for sample traces). Pairwise *t*-tests were conducted comparing the slow currents recorded at +80 and −80 mV in the same cells. There was no significant effect of voltage on the currents evoked by 4OH-GTS-21. However, for currents evoked by ACh, there was proportionately more slow current recorded at +80 mV than at −80 mV (* $P<0.05$).

concentration ramp. If that is the case, then the fully-liganded state cannot have the highest probability of opening, as was proposed for α7-type responses in cultured hippocampal neurons [20].

We have previously proposed that the pronged activation of TM neuronal α7-type receptors observed after agonist removal might be due to an association of maximal P_{open} with a submaximal level of agonist occupancy [23]. This 'partial occupancy model' does predict the agonist concentration dependence of the fast desensitization. The partial occupancy model also predicts that once the cell is removed from the agonist stream, the average level of agonist occupancy would progressively decrease, so that more channels would return to the level of occupancy most likely to promote channel opening upon agonist removal. In this way, our previous model [23] explicitly predicted the rebound current which was experimentally observed for 4OH-GTS-21. The model also predicted the bell-shaped concentration–response function we observe. However, while the partial occupancy model can be used to fit the 4OH-GTS-21 at all voltages, since rebound is consistently observed, efforts to fit the rebound-free ACh data recorded at positive potentials to that model have not been successful (Uteshev, unpublished data). Therefore, if the 4OH-GTS-21 rebound currents do arise from the relief of a channel block, analogous to that produced by ACh and choline, then the partial occupancy model is unlikely to be correct.

An alternative hypothesis which might explain the concentration dependence of the fast desensitization would be that desensitization rates vary for different levels of agonist occupancy, such that the desensitization rate of fully-liganded receptors is nearly instantaneous (or at least much faster than the corresponding opening rate). A similar model with desensitization rates varying with the level of agonist occupancy has been proposed for the structurally related homomeric 5HT3a receptors [21], although for that receptor the rate constants that fit the model for 5HT3a receptors are all very slow. Accelerated

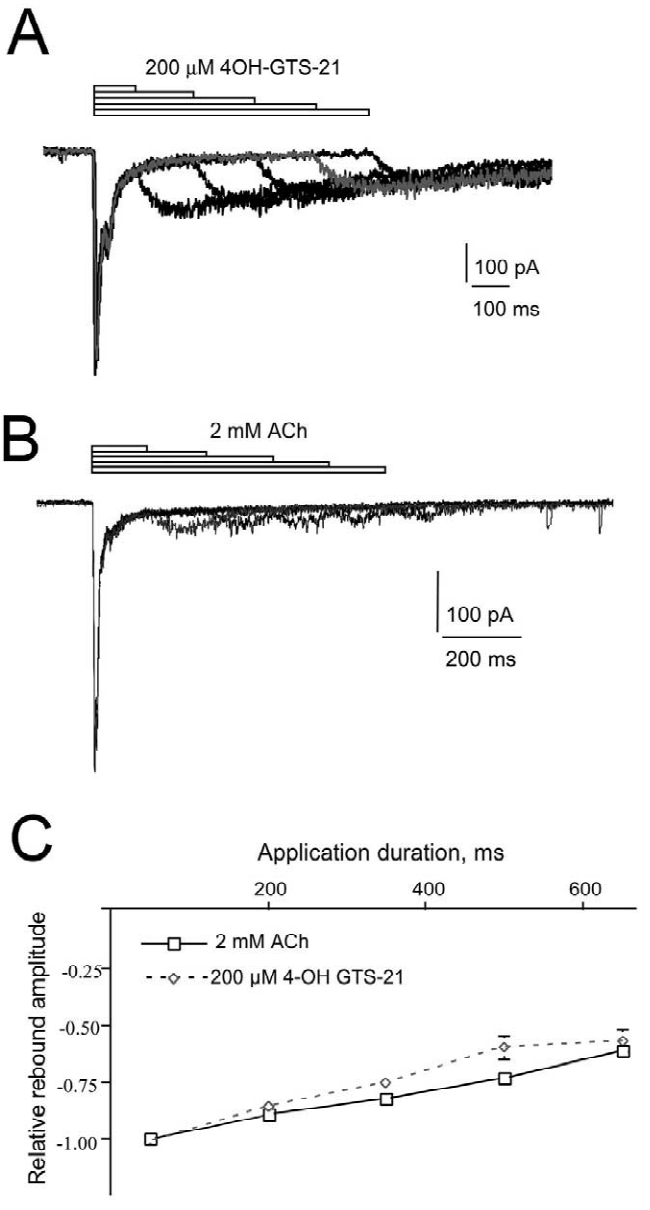

Fig. 8. (A) Transient responses and rebound currents for 4OH-GTS-21 applications of varying duration to a TM neuron. The bars above the current traces represent the application durations tested. The amplitudes of the current rebounds in the 4OH-GTS-21-evoked responses were inversely dependent on the 4OH-GTS-21 application duration time; longer application produced smaller current rebounds. Note that for 4OH-GTS-21, the rebounds corresponding to longer duration applications were embraced by rebounds produced by shorter applications, suggesting that the rate of slow desensitization was similar to or identical to the rate that determines the decay of each individual rebound current. (B) Transient responses and rebound currents for ACh applications of varying duration to a TM neuron. Note that when 2 mM ACh was applied for longer durations, there was a progressive decrease in the amplitude of the rebound current, but the decay of each individual rebound current was fast compared to the decay of the 4OH-GTS-21-evoked rebound currents (Fig. 6). (C) Average of peak amplitudes (±S.E.M.) of relative rebound currents following ACh ($n=3$) and 4OH-GTS-21 ($n=4$) applications of varying duration. Rebound amplitudes for progressively longer agonist applications were normalized to the rebound amplitude obtained with a 50-ms application in the same cell. Note that the rate at which channels became unavailable for rebound current was similar for both ACh and 4OH-GTS-21 (time constants of 1264 and 1010 ms, respectively), suggesting that although the decay rates of the individual rebound currents depended upon which agonist was used, the slow desensitization rate for fully liganded channels, which made channels unavailable for rebound, was similar for both agonists.

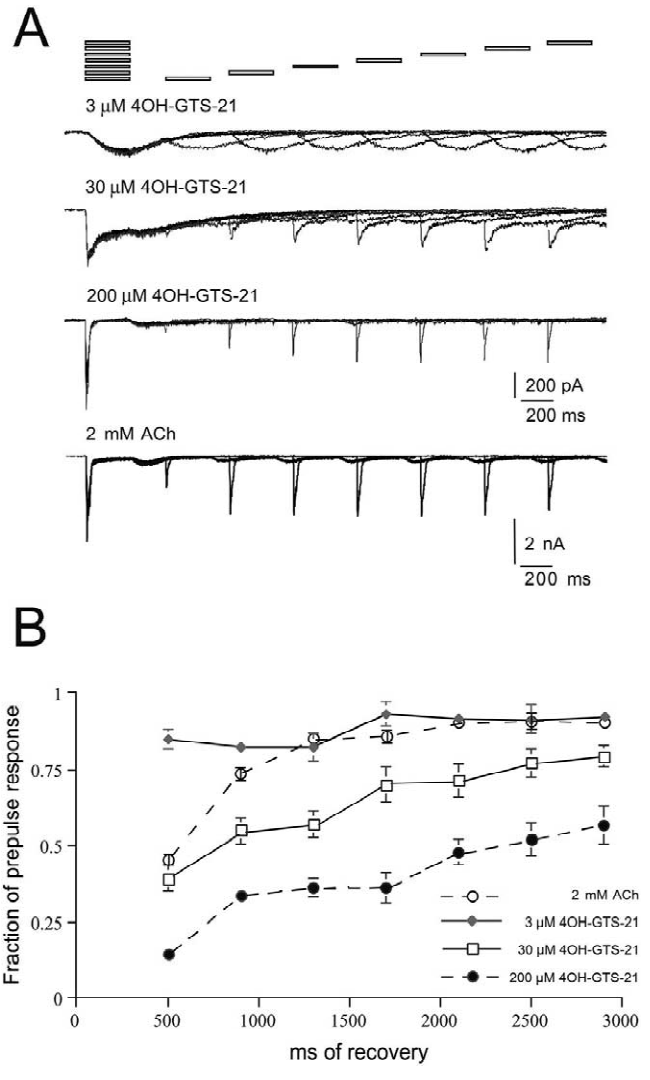

Fig. 9. (A) Examples of typical traces from pair-pulse experiments with different concentrations of 4OH-GTS-21 and 2 mM ACh. Responses to applications of low 4OH-GTS-21 concentrations demonstrated faster recovery from desensitization than responses to applications of higher concentrations of 4OH-GTS-21. However, all responses were completely recovered in 40 s, the interval between subsequent pair-pulse trains. Responses to 2 mM ACh recovered rapidly, presumably due to a faster unbinding rate of ACh compared to 4OH-GTS-21. (B) The averaged recovery from desensitization estimated over several experiments from different TM neurons ($n=5$).

desensitization of fully-liganded receptors does not predict rebound currents, which is consistent with the hypothesis that rebound currents can be attributed strictly to the relief of channel block.

Whether the fast desensitization of α7 receptors represents classical (i.e. first order) desensitization or a pseudo first-order concentration-driven process, it was seen to relax to the level associated with the slow current. At relatively low agonist concentrations (e.g. 3 μM 4OH-GTS-21), there was no apparent fast desensitization, and the slow current was sustained over the time scale of our recordings. During the prolonged application of relatively high agonist concentrations, there was a small decay in the slow current, which would seem to represent another form of desensitization. It is this process which limits the amount of delayed current. The channel block occurring during the slow current was readily reversed when the cell was removed from the agonist stream, with the relief of inhibition manifested as the rebound current. Rebound currents then rose to the same level as that seen as the maximal possible slow and delayed currents obtained with lower concentrations of agonist, e.g. 10–30 μM 4OH-GTS-21 or 200 μM ACh. In the case of ACh, these levels of slow current were the same as those produced by high concentrations of ACh when recordings were made at positive potentials so that the influence of channel block was minimized. In the case of 4OH-GTS-21, the delayed current saturated above 30 μM 4OH-GTS-21 and the slow current was voltage-independent. These observations are consistent with the hypothesis that channel block is superimposed on the progress of a slow desensitization which would otherwise be limiting.

The decay rate of the delayed current is a kinetic feature which seems strongly dependent on the nature of the agonist. For ACh and choline, this decay rate may represent the rate at which agonist dissociates from the activation sites which were promoting the slow current. However, since the decay rate of the 4OH-GTS-21 delayed current was the same as the slow desensitization rate (Fig. 8A) (which appeared to be the same for both ACh and 4OH-GTS-21, Fig. 8C) it is likely that 4OH-GTS-21 dissociated more slowly than or equal to the rate for slow desensitization, so that slow desensitization continued to increase during the 4OH-GTS-21 delayed current. This is consistent with the observation that there was more complete desensitization after a 4OH-GTS-21 delayed current than after an ACh or choline-associated delayed current. Although 2 mM ACh and 30 μM 4OH-GTS-21 produced the same amount of desensitization measured after a 500-ms wash, when ACh was the agonist used to produce the desensitization, the recovery rate was at least twice as fast as when 4OH-GTS-21 was the agonist (Fig. 9).

The α7 nicotinic receptor appears to be the target for recently developed memory-enhancing and neuroprotective agents such as GTS-21 and 4OH-GTS-21 [23,24], which are being evaluated clinically for the treatment of Alzheimer's disease [14]. These compounds are selective partial agonists of α7 nicotinic receptors [18] and as such have the capacity to induce a variety of calcium-sensitive intracellular transduction processes that differ depending on the agonist concentration [16]. In this paper, we provide data which indicates that activation of the receptor by low agonist concentrations may represent an important functional modality of α7 receptors. Functioning in this mode, α7 receptors may flux calcium and regulate calcium homeostasis over a narrow but physiologically important range of intracellular calcium concentrations. This could

then provide the basis for cytoprotective effects of nicotinic agonists. While large increases in intracellular calcium have been reported to be cytotoxic, relatively small increases in calcium, such as would be associated with tonic but small levels of α7 receptor activation, are known to be cytoprotective. This has given rise to the calcium-set-point hypothesis of neuroprotection [11]. It has also been shown that small αBgt-sensitive increases in the intracellular calcium concentration of synaptic terminals have been demonstrated under conditions when low concentrations of nicotine produce increases in transmitter release probability [10,17]. Consistent with the concept that low levels of essentially steady-state activation may be important for the role of the α7 receptor in regulating calcium homeostasis is the suggestion that choline may be an important activator of this receptor in the brain. Choline selectively activates α7 receptors [22] and is normally present in the cerebral spinal fluid at concentrations of around 10–20 μM [15]. However, choline can rise to the range of 100 μM with trauma or other insult [12,25]. Our data suggest that 100 μM choline would be in the range that might optimally produce tonic activation of α7-type receptors. Likewise, the optimal cytoprotective effects of therapeutic ligands such as 4OH-GTS-21 lie in the range of 1–3 μM [16]. This is the range in which 4OH-GTS-21 was most effective at stimulating net charge between 500 and 1000 ms after initial application. Our observations therefore support the idea that α7 receptors in the CNS are well suited for tonic activity, mediating trophic and neuromodulatory functions, as well as representing a target for treating neurodegenerative disorders such as Alzheimer's disease.

Acknowledgements

We thank Dr James Dilger for his suggestion to use low Na solution for the measurements of solution exchange kinetics. We thank Drs Peter Pennefather, Steve Traynelis and Robert Oswald for helpful discussions and Dr Charles J. Frazier and Clare Stokes for comments on the manuscript. We thank Taiho Pharmaceuticals for providing 4OH-GTS-21. This work was supported by NIH grants NS32888-02 and GM57481-01A2.

References

[1] M. Alkondon, E.X. Albuquerque, Diversity of nicotinic acetylcholine receptors in rat hippocampal neurons. I. Pharmacological and functional evidence for distinct structural subtypes, J. Pharmacol. Exp. Ther. 265 (1993) 1455–1473.

[2] M. Alkondon, E.F. Pereira, E.X. Albuquerque, Alpha-bungarotoxin- and methyllycaconitine-sensitive nicotinic receptors mediate fast synaptic transmission in interneurons of rat hippocampal slices, Brain Res. 810 (1998) 257–263.

[3] M. Alkondon, E.F. Pereira, W.S. Cortes, A. Maelicke, E.X. Albuquerque, Choline is a selective agonist of alpha7 nicotinic acetylcholine receptors in the rat brain neurons, Eur. J. Neurosci. 9 (1997) 2734–2742.

[4] M. Alkondon, S. Reinhardt, C. Lobron, B. Hermsen, A. Maelicke, E.X. Albuquerque, Diversity of nicotinic acetylcholine receptors in rat hippocampal neurons. II. The rundown and inward rectification of agonist-elicited whole cell currents and identification of receptor subunits by in situ hybridization, J. Phamacol. Exp. Ther. 271 (1994) 494–506.

[5] M. Alkondon, E.S. Rocha, A. Maelicke, E.X. Albuquerque, Diversity of nicotinic acetylcholine receptors in rat brain. V. α-Bungarotoxin-sensitive nicotinic receptors in olfactory bulb neurons and presynaptic modulation of glutamate release, J. Pharmacol. Exp. Ther. 278 (1996) 1460–1471.

[6] P.B.S. Clarke, R.D. Schwartz, S.M. Paul, C.B. Pert, A. Pert, Nicotinic binding in rat brain: autoradiographic comparison of [^{3}H]acetylcholine, [$_{3}$H]nicotine and [^{125}I]alpha-bungarotoxin, J. Neurosci. 5 (1985) 1307–1315.

[7] R.C. Drisdel, W.N. Green, Neuronal alpha-bungarotoxin receptors are alpha7 subunit homomers, J. Neurosci. 20 (2000) 133–139.

[8] M.M. Francis, K.I. Choi, B.A. Horenstein, R.L. Papke, Sensitivity to voltage-independent inhibition determined by pore-lining region of ACh receptor, Biophys. J. 74 (1998) 2306–2317.

[9] C.J. Frazier, A.V. Buhler, J.L. Weiner, T.V. Dunwiddie, Synaptic potentials mediated via α-bungarotoxin-sensitive nicotinic acetylcholine receptors in rat hippocampal interneurons, J. Neurosci. 18 (1998) 8228–8235.

[10] R. Gray, A.S. Rajan, K.A. Radcliffe, M. Yakehiro, J.A. Dani, Hippocampal synaptic transmission enhanced by low concentrations of nicotine, Nature 383 (1996) 713–716.

[11] J. Johnson, T. Koike, J. Franklin, A 'calcium set-point hypothesis' of neuronal dependence on neurotrophic factor, Exp. Neurol. 115 (1992) 163–166.

[12] R.S. Jope, X. Gu, Seizures increase acetylcholine and choline concentrations in rat brain regions, Neurochem. Res. 16 (1991) 1219–1226.

[13] A.Y. Kabakov, R.L. Papke, Ultra fast solution applications for prolonged gap-free recordings: Controlling a Burleigh piezo-electric positioner with Clampex7, Axobits (January) (1998) 6–9.

[14] H. Kitagawa, T. Takenouchi, K. Wesnes, W. Kramer, D.E. Clody, Phase I studies of GTS-21 to assess the safety, tolerability, PK, and effects on measures of cognitive function in normal volunteers, in: 6th International Conference on Alzheimer's Disease, 1998, abstract 765.

[15] J. Klein, A. Koppen, K. Loffelholz, J. Schmitthenner, Uptake and metabolism of choline by rat brain after acute choline administration, J. Neurochem. 58 (1992) 870–876.

[16] Y. Li, R.L. Papke, Y.-J. He, B. Millard, E.M. Meyer, Characterization of the neuroprotective and toxic effects of α7 nicotinic receptor activation in PC12 cells, Brain Res. 81 (1999) 218–225.

[17] D.S. McGehee, M.J.S. Heath, S. Gelber, P. Devay, L.W. Role, Nicotine enhancement of fast excitatory synaptic transmission in CNS by presynaptic receptors, Science 269 (1995) 1692–1696.

[18] E. Meyer, A. Kuryatov, V. Gerzanich, J. Lindstrom, R.L. Papke, Analysis of 4OH-GTS-21 selectivity and activity at human and rat α7 nicotinic receptors, J. Pharmacol. Exp. Ther. 287 (1998) 918–925.

[19] E.M. Meyer, E.T. Tay, R.L. Papke, C. Meyers, G. Huang, C.M. de Fiebre, Effects of 3-[2,4-dimethoxybenzylidene]anabaseine (DMXB) on rat nicotinic receptors and memory-related behaviors, Brain Res. 768 (1997) 49–56.

[20] A. Mike, N.G. Castro, E.X. Albuquerque, Choline and acetylcholine have similar kinetic properties of activation and desensitization on the alpha7 nicotinic receptors in rat hippocampal neurons, Brain Res. 882 (2000) 155–168.

[21] D.D. Mott, K. Erreger, T.G. Banke, S.F. Traynelis, Open probability of homomeric murine 5-HT(3A) serotonin receptors depends on subunit occupancy, J. Physiol. 535 (2001) 427–443.

[22] R.L. Papke, M. Bencherif, P. Lippiello, An evaluation of neuronal nicotinic acetylcholine receptor activation by quaternary nitrogen compounds indicates that choline is selective for the α7 subtype, Neurosci. Lett. 213 (1996) 201–204.
[23] R.L. Papke, E. Meyer, T. Nutter, V.V. Uteshev, Alpha7-selective agonists and modes of alpha7 receptor activation, Eur. J. Pharm. 393 (2000) 179–195.
[24] R.L. Papke, J.S. Thinschmidt, The correction of alpha7 nicotinic acetylcholine receptor concentration–response relationships in *Xenopus* oocytes, Neurosci. Lett. 256 (1998) 163–166.
[25] O.U. Scremin, D.J. Jenden, Time-dependent changes in cerebral choline and acetylcholine induced by transient global ischemia in rats, Stroke 22 (1991) 643–647.
[26] V. Uteshev, D.R. Stevens, H.L. Haas, A persistent sodium current in acutely isolated histaminergic neurons from rat hypothalamus, Neuroscience 66 (1995) 143–149.
[27] V.V. Uteshev, D.R. Stevens, H.L. Haas, alpha-Bungarotoxin-sensitive nicotinic responses in rat tuberomammillary neurons, Eur. J. Physiol. 432 (1996) 607–613.